

Controllable four-wave mixing response in a dual-cavity hybrid optomechanical system

Lei Shang(尚蕾), Bin Chen(陈彬), Li-Li Xing(邢丽丽), Jian-Bin Chen(陈建宾), Hai-Bin Xue(薛海斌), Kang-Xian Guo(郭康贤)

Citation: Chin. Phys. B, 2021, 30 (**5**): 054209. DOI: 10.1088/1674-1056/abd695
Journal homepage: http://cpb.iphy.ac.cn; http://iopscience.iop.org/cpb

What follows is a list of articles you may be interested in

Quantum plasmon enhanced nonlinear wave mixing in graphene nanoflakes

Hanying Deng(邓寒英), Changming Huang(黄长明), Yingji He(何影记), and Fangwei Ye(叶芳伟)
Chin. Phys. B, 2021, 30 (**4**): 044213. DOI: 10.1088/1674-1056/abea8d

A two-mode squeezed light based on a double-pump phase-matching geometry

Xuan-Jian He(何烜坚), Jun Jia(贾俊), Gao-Feng Jiao(焦高锋), Li-Qing Chen(陈丽清), Chun-Hua Yuan(袁春华), Wei-Ping Zhang(张卫平)
Chin. Phys. B, 2020, 29 (**7**): 074207. DOI: 10.1088/1674-1056/ab8abd

Light slowing and all-optical time division multiplexing of hybrid four-wave mixing signal in nitrogen-vacancy center

Ruimin Wang(王瑞敏), Irfan Ahmed, Faizan Raza, Changbiao Li(李昌彪), Yanpeng Zhang(张彦鹏)
Chin. Phys. B, 2020, 29 (**5**): 054204. DOI: 10.1088/1674-1056/ab7b50

Electro-optomechanical switch via tunable bistability and four-wave mixing

Kamran Ullah
Chin. Phys. B, 2019, 28 (**11**): 114209. DOI: 10.1088/1674-1056/ab4580

Simultaneous polarization separation and switching for 100-Gbps DP-QPSK signals in backbone networks

Yu-Long Su(苏玉龙), Huan Feng(冯欢), Hui Hu(胡辉), Wei Wang(汪伟), Tao Duan(段弢), Yi-Shan Wang(王屹山), Jin-Hai Si(司金海), Xiao-Ping Xie(谢小平), He-Ning Yang(杨合宁), Xin-Ning Huang(黄新宁)
Chin. Phys. B, 2019, 28 (**2**): 024216. DOI: 10.1088/1674-1056/28/2/024216

Controllable four-wave mixing response in a dual-cavity hybrid optomechanical system*

Lei Shang(尚蕾)[1], Bin Chen(陈彬)[1,2,†], Li-Li Xing(邢丽丽)[1], Jian-Bin Chen(陈建宾)[1], Hai-Bin Xue(薛海斌)[1], and Kang-Xian Guo(郭康贤)[3]

[1] *Department of Physics, College of Physics and Optoelectronics, Taiyuan University of Technology, Taiyuan* 030024, *China*
[2] *Key Laboratory of Advanced Transducers and Intelligent Control System, Ministry of Education and Shanxi Province, Taiyuan* 030024, *China*
[3] *Department of Physics, School of Physics and Material Science, Guangzhou University, Guangzhou* 510006, *China*

(Received 10 November 2020; revised manuscript received 14 December 2020; accepted manuscript online 24 December 2020)

We systematically investigate the four-wave mixing (FWM) spectrum in a dual-cavity hybrid optomechanical system, which is made up of one optical cavity with an ensemble of two-level atoms and another with a mechanical oscillator. In this work, we propose that the hybrid dual-cavity optomechanical system can be employed as a highly sensitive mass sensor due to the fact that the FWM spectrum generated in this system has a narrow spectral width and the intensity of the FWM can be easily tuned by controlling the coupling strength (cavity–cavity, atom–cavity). More fascinatingly, the dual-cavity hybrid optomechanical system can also be used as an all-optical switch in view of the easy on/off control of FWM signals by adjusting the atom-pump detuning to be positive or negative. The proposed schemes have great potential applications in quantum information processing and highly sensitive detection.

Keywords: four-wave mixing, dual-cavity optomechanical system, atomic ensemble

PACS: 42.50.Ct, 42.50.−p, 42.65.−k **DOI:** 10.1088/1674-1056/abd695

1. Introduction

In the past few decades, the nonlinear optical effects[1] caused by the interaction between light and matter have been a striking research topic and optomechanical systems,[2–10] as a good platform for studying nonlinear optical effects, have received a great deal of attention. The most typical optomechanical system is composed of an optical cavity with a mechanical resonator. Recently, researchers have extended single-cavity optomechanical systems to hybrid cavity optomechanical systems[11–18] by coupling more optical or mechanical modes, such as an atomic ensemble, a quantum well, a Kerr medium or other media with optomechanical cavities. More optical effects, such as electromagnetically induced transparency,[19–26] optical bistability,[27–31] slow light effects[32–37] and so on, have been extensively explored in these hybrid systems.

Currently, the four-wave mixing (FWM) effect,[37–49] one of the classic nonlinear effects, is widely studied in optomechanical systems. Jiang *et al.*[37] investigated how to control the FWM process in a two-mode cavity optomechanical system. In a three-mode optomechanical system with atom–cavity mirror coupling, Wang and Chen[39] confirmed that the FWM response can be well enhanced. In a composite photonic-molecule optomechanical system, Chen *et al.*[40] studied the process of normal mode splitting in the FWM spectrum under different parameter and driving conditions. Li *et al.*[41] realized multimode FWM in an unresolved sideband optomechanical system.

Inspired by the above work, we explore the FWM process in a hybrid dual-cavity optomechanical system with cavity A containing an ensemble of two-level atoms and cavity B coupling a mechanical oscillator. We mainly pay attention to the FWM effect in cavity B and investigate the dependence of the FWM on system parameters such as pump power, coupling strength, detuning, etc. Here, we propose a scheme in which this optomechanical system can serve as an optical mass sensor and an all-optical switch based on measurement of the FWM spectrum. These schemes are important for potential applications of this hybrid system in quantum information processing or highly sensitive detection. The structure of this paper is as follows: In Section 2, the theoretical model and theoretical calculation of the equation are introduced. Section 3 focuses on the analysis and discussion of the results. Section 4 presents a summary.

2. Theoretical model

As depicted schematically in Fig. 1, the dual-cavity hybrid optomechanical system considered in this paper is composed of optical cavity A containing an atomic ensemble and cavity B interacting with a mechanical oscillator.

*Project supported by the National Natural Science Foundation of China (Grant Nos. 11504258, 61775043, and 11805140) and the Natural Science Foundation of Shanxi Province, China (Grant Nos. 201801D221021 and 201801D221031).

†Corresponding author. E-mail: chenbin@tyut.edu.cn

© 2021 Chinese Physical Society and IOP Publishing Ltd

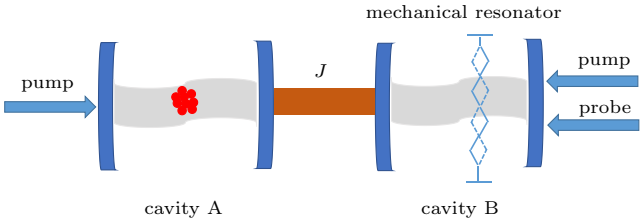


Fig. 1. Schematic of a dual-cavity hybrid optomechanical system, where two cavities have identical lengths L and mode frequencies $\omega_{\rm c}$.

These two cavities are coupled with each other via an evanescent field and the coupling strength is denoted as J. In addition, cavity A is driven by a strong pump light with frequency $\omega_{\rm p1}$ and amplitude $\varepsilon_{\rm p1}$, while a strong pump light with frequency $\omega_{\rm p2}$ and amplitude $\varepsilon_{\rm p2}$ as well as a weak probe light with frequency $\omega_{\rm pr}$ and amplitude $\varepsilon_{\rm pr}$ are applied to cavity B. For simplicity, the frequency $\omega_{\rm p1}$ is chosen to be the same as $\omega_{\rm p2}$, and cavities A and B are assumed to have the same mode frequency $\omega_{\rm c}$. In a frame rotating at $\omega_{\rm p2}$, the Hamiltonian of this system can be written as follows:

$$\begin{aligned} H \;=\; & \hbar\Delta_{\rm c}a^{\dagger}a+\hbar\Delta_{\rm c}b^{\dagger}b+\hbar J(a^{\dagger}b+b^{\dagger}a) \\ & +\frac{1}{2}\hbar\omega_{\rm m}(x^2+p^2)+\hbar g_0 b^{\dagger}bx \\ & +\sum_{i=1}^{N}\hbar\Delta_a\sigma_{\rm ee}^{(i)}+\hbar g_a\sum_{i=1}^{N}\left(a\,\sigma_{\rm eg}^{(i)}+a^{\dagger}\sigma_{\rm ge}^{(i)}\right) \\ & +{\rm i}\hbar\varepsilon_{\rm p1}(a^{\dagger}-a)+{\rm i}\hbar\varepsilon_{\rm p2}(b^{\dagger}-b) \\ & +{\rm i}\hbar\varepsilon_{\rm pr}(b^{\dagger}{\rm e}^{-{\rm i}\delta t}-b\,{\rm e}^{{\rm i}\delta t}). \end{aligned} \tag{1}$$

In Eq. (1), the first three terms, respectively, represent the energy of cavities A and B, and their coupling interactions. Here, $\Delta_{\rm c}=\omega_{\rm c}-\omega_{\rm p2}$ is the cavity-pump detuning. a (b) and $a^{\dagger}$ ($b^{\dagger}$) are, respectively, the annihilation and generation operators of cavity A (B), satisfying the commutation relation $\left[a,a^{\dagger}\right]=1$ and $\left[b,b^{\dagger}\right]=1$. The fourth and fifth terms, respectively, give the energy of the mechanical oscillator and its coupling interaction with cavity A, where $\omega_{\rm m}$ is the frequency of the mechanical resonator, x and p are dimensionless displacement and momentum operators, and $g_0=(\omega_{\rm c}/L)\sqrt{\hbar/m\omega_{\rm m}}$ is the coupling strength between the cavity with the length L and the mechanical resonator with mass m. The sixth and seventh terms, respectively, show the energy of the atomic ensemble and its interaction with cavity B, where Δ_a is a single atom-pump detuning and g_a is the coupling strength between the atomic ensemble and cavity modes. The last three terms describe the interactions of the cavity field with the external driving field ε_i, where $\varepsilon_i=\sqrt{2\kappa P_i/\hbar\omega_i},(i={\rm p1,p2,pr})$, κ is the cavity decay rate, and $\delta=\omega_{\rm pr}-\omega_{\rm p2}$ is the probe-pump detuning.

In the case where the total number of atoms N is large enough and all the atoms can be considered as a whole, a collective atomic operator can be defined as $A=\frac{1}{\sqrt{N}}\sum_{i=1}^{N}\sigma_{\rm ge}^{(i)}$ satisfying the bosonic commutation relation $\left[A,A^{\dagger}\right]=1$ with $\sigma_{\rm ge}^{(i)}=|g\rangle_i\langle e|$ symbolizing the ith atomic transition operator. With the introduction of the collective atomic operator A, the Hamiltonian can be expressed as

$$\begin{aligned} H \;=\; & \hbar\Delta_{\rm c}a^{\dagger}a+\hbar\Delta_{\rm c}b^{\dagger}b+\hbar J(a^{\dagger}b+b^{\dagger}a)+\frac{1}{2}\hbar\omega_{\rm m}(x^2+p^2) \\ & +\hbar g_0 b^{\dagger}bx+\hbar\Delta_a A^{\dagger}A+\hbar G(aA^{\dagger}+a^{\dagger}A)+{\rm i}\hbar\varepsilon_{\rm p1}(a^{\dagger}-a) \\ & +{\rm i}\hbar\varepsilon_{\rm p2}(b^{\dagger}-b)+{\rm i}\hbar\varepsilon_{\rm pr}(b^{\dagger}{\rm e}^{-{\rm i}\delta t}-b\,{\rm e}^{{\rm i}\delta t}), \end{aligned} \tag{2}$$

where $G=g_a\sqrt{N}$ signifies the coupling strength between the cavity and the total atoms, which can be modified through changing the number of atoms. Here, we mainly focus on the mean response of the probe field to the hybrid dual-cavity optomechanical system. According to the Heisenberg equations $\frac{{\rm d}A}{{\rm d}t}=\frac{1}{{\rm i}\hbar}[A(t),H]$ and the corresponding commutation relation, we can obtain the equations for the mean value of the operators x, p, a, b, A as follows by using the same method as the references:[20,21]

$$\begin{aligned} \dot{x} \;&=\; \omega_{\rm m}p, \\ \dot{p} \;&=\; -\omega_{\rm m}x+g_0b^{\dagger}b-\gamma_{\rm m}p, \\ \dot{a} \;&=\; -{\rm i}\Delta_{\rm c}a-{\rm i}Jb-{\rm i}GA+\varepsilon_{\rm p1}-\kappa a, \\ \dot{b} \;&=\; -{\rm i}\Delta_{\rm c}b-{\rm i}Ja-{\rm i}g_0bx+\varepsilon_{\rm pr}{\rm e}^{-{\rm i}\delta t}+\varepsilon_{\rm p2}-\kappa b, \\ \dot{A} \;&=\; -({\rm i}\Delta_a+\gamma_a)A-{\rm i}Ga. \end{aligned} \tag{3}$$

In Eq. (3), we phenomenologically add the cavity decay rate κ, the atomic coherence decay rate γ_a and the damping rate of the mechanical oscillator $\gamma_{\rm m}$, and ignore quantum and thermal noise terms. To solve the above equations, we make the following ansatz:

$$\begin{aligned} x \;&=\; x_0+x_+{\rm e}^{-{\rm i}\delta t}+x_-{\rm e}^{{\rm i}\delta t}, \\ p \;&=\; p_0+p_+{\rm e}^{-{\rm i}\delta t}+p_-{\rm e}^{{\rm i}\delta t}, \\ a \;&=\; a_0+a_+{\rm e}^{-{\rm i}\delta t}+a_-{\rm e}^{{\rm i}\delta t}, \\ b \;&=\; b_0+b_+{\rm e}^{-{\rm i}\delta t}+b_-{\rm e}^{{\rm i}\delta t}, \\ A \;&=\; A_0+A_+{\rm e}^{-{\rm i}\delta t}+A_-{\rm e}^{{\rm i}\delta t}, \end{aligned} \tag{4}$$

where x_0, p_0, a_0, b_0, A_0 are, respectively, the steady-state solutions of x, p, a, b, A. By substituting Eq. (4) into Eq. (3) and solving these equations, we can get

$$\begin{aligned} x_0 \;&=\; -\frac{g_0|b_0|^2}{\omega_{\rm m}}, \\ p_0 \;&=\; 0, \\ a_0 \;&=\; \frac{\varepsilon_{\rm p1}-{\rm i}Jb_0-{\rm i}GA_0}{{\rm i}\Delta_{\rm c}+\kappa}, \\ A_0 \;&=\; \frac{-{\rm i}Ga_0}{\gamma_a+{\rm i}\Delta_a}, \\ b_0 \;&=\; \frac{\varepsilon_{\rm p2}-{\rm i}Ja_0}{{\rm i}\Delta_{\rm c}+{\rm i}g_0x_0+\kappa}, \\ b_- \;&=\; \frac{B_1\varepsilon_{\rm pr}}{(D_1+E_1+B_0)(D_2+E_2-B_0)+B_1B_2^{*}}, \end{aligned} \tag{5}$$

with

$$
\begin{aligned}
B_0 &= \frac{\omega_{\rm m} {g_0}^2 |b_0|^2}{(\gamma_{\rm m}+{\rm i}\delta)\,\delta-{\rm i}\omega_{\rm m}^2},\\
B_1 &= \frac{\omega_{\rm m} {g_0}^2 {b_0}^2}{(\gamma_{\rm m}+{\rm i}\delta)\,\delta-{\rm i}\omega_{\rm m}^2},\\
B_2 &= \frac{\omega_{\rm m} {g_0}^2 {b_0}^2}{(-\gamma_{\rm m}+{\rm i}\delta)\,\delta+{\rm i}\omega_{\rm m}^2},\\
D_1 &= {\rm i}\delta-{\rm i}\,(\Delta_{\rm c}+g_0 x_0)+\kappa,\\
D_2 &= {\rm i}\delta+{\rm i}\,(\Delta_{\rm c}+g_0 x_0)+\kappa,\\
E_1 &= \frac{J^2}{-{\rm i}\Delta_{\rm c}+{\rm i}\delta+\kappa+\left(\frac{G^2}{{\rm i}\delta-{\rm i}\Delta_a+\gamma_a}\right)},\\
E_2 &= \frac{J^2}{{\rm i}\Delta_{\rm c}+{\rm i}\delta+\kappa+\left(\frac{G^2}{{\rm i}\delta+{\rm i}\Delta_a+\gamma_a}\right)}.
\end{aligned}
\tag{6}
$$

Here, b_- denotes the amplitude of the FWM generated in this dual-cavity hybrid optomechanical system, which we are interested in. Utilizing the input–output relationship[50,51] $b_{\rm out}(t)=b_{\rm in}(t)-\sqrt{2\kappa}b(t)$. The output field from cavity B can be given by

$$
\begin{aligned}
b_{\rm out}(t) &= (\varepsilon_{\rm p2}/\sqrt{2\kappa}-\sqrt{2\kappa}b_0){\rm e}^{-{\rm i}\omega_{\rm p2}t}\\
&\quad+(\varepsilon_{\rm pr}/\sqrt{2\kappa}-\sqrt{2\kappa}b_+){\rm e}^{-{\rm i}(\delta+\omega_{\rm p2})t}\\
&\quad-\sqrt{2\kappa}b_-{\rm e}^{{\rm i}(\delta-\omega_{\rm p2})t}\\
&= (\varepsilon_{\rm p2}/\sqrt{2\kappa}-\sqrt{2\kappa}b_0){\rm e}^{-{\rm i}\omega_{\rm p2}t}\\
&\quad+(\varepsilon_{\rm pr}/\sqrt{2\kappa}-\sqrt{2\kappa}b_+){\rm e}^{-{\rm i}\omega_{\rm pr}t}\\
&\quad-\sqrt{2\kappa}b_-{\rm e}^{-{\rm i}(2\omega_{\rm p2}-\omega_{\rm pr})t},
\end{aligned}
\tag{7}
$$

where the first two terms in Eq. (7), respectively, describe the output fields at frequencies $\omega_{\rm p2}$ and $\omega_{\rm pr}$ while the last term depicts an output field of FWM.

A relative output field intensity of FWM from cavity B can be defined in terms of the probe field as follows:

$$
I_{\rm FWM}=\left|\frac{-\sqrt{2\kappa}b_-}{\varepsilon_{\rm pr}/\sqrt{2\kappa}}\right|^2=\left|\frac{2\kappa b_-}{\varepsilon_{\rm pr}}\right|^2. \tag{8}
$$

3. Results and discussion

In order to reveal the FWM process more concisely, we choose the realistic experimental parameters of the dual-cavity hybrid system[37,39] as $\lambda=1064$ nm, $l=1.5$ mm, $m=10$ ng, $\omega_{\rm m}=2\pi\times10$ MHz, $\kappa=2\pi\times1$ MHz, $\gamma_{\rm m}=2\pi\times100$ Hz, $\gamma_a=2\pi\times5$ MHz, $\Delta_a=-1.0\omega_{\rm m}$, $\Delta_{\rm c}=1.0\omega_{\rm m}$.

Figure 2 shows the FWM intensity $I_{\rm FWM}$ as a function of the probe-pump detuning $\delta/\omega_{\rm m}$ for two different pump schemes. As is shown in Fig. 2(a), when the left pump laser is off ($P_{\rm p1}=0$) but the right one is on, two strong peaks appear at $\delta\sim\pm\omega_{\rm m}$ in the FWM spectrum, which exactly correspond to the vibrational frequency of the mechanical oscillator. Most interestingly, for the opposite pump schemes, i.e., the left pump laser on and the right one off ($P_{\rm p2}=0$), the two FWM peaks at $\delta\sim\pm\omega_{\rm m}$ become much narrower as shown in Fig. 2(b), while their intensity only suffers a small reduction. These important results demonstrate that this dual-cavity hybrid optomechanical system can be used as a sensitive quantum sensor, for example as a mass sensor,[52] when it is only driven by a left pump laser. It is well known that, for a quantum sensor, the spectrum width is an important factor affecting its sensitivity.[52] The narrower the spectral width is, the more high resolution of the sensor will be. Taking the mass sensor proposed in the reference[52] as an example, its sensitivity and resolution could be significantly enhanced by introducing a plasma into the system as the probe spectrum width was modulated effectively.

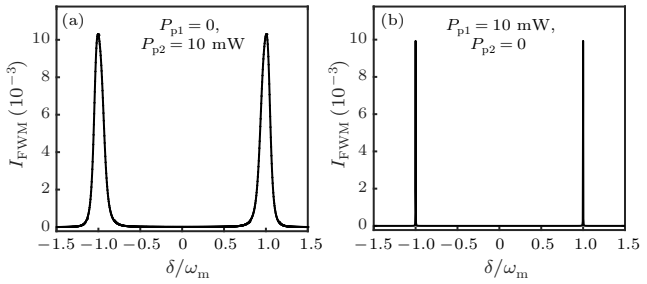


Fig. 2. The FWM intensity $I_{\rm FWM}$ as a function of the probe-pump detuning $\delta/\omega_{\rm m}$ for the case: (a) $P_{\rm p1}=0$ and $P_{\rm p2}=10$ mW, (b) $P_{\rm p1}=10$ mW and $P_{\rm p2}=0$. The other parameters are taken as $\lambda=1064$ nm, $l=1.5$ mm, $m=10$ ng, $\omega_{\rm m}=2\pi\times10$ MHz, $\kappa=2\pi\times1$ MHz, $\gamma_{\rm m}=2\pi\times100$ Hz, $\gamma_a=2\pi\times5$ MHz, $\Delta_a=-1.0\omega_{\rm m}$, $\Delta_{\rm c}=1.0\omega_{\rm m}$, $G=2\pi\times5$ MHz, $J=2\pi\times1$ MHz.

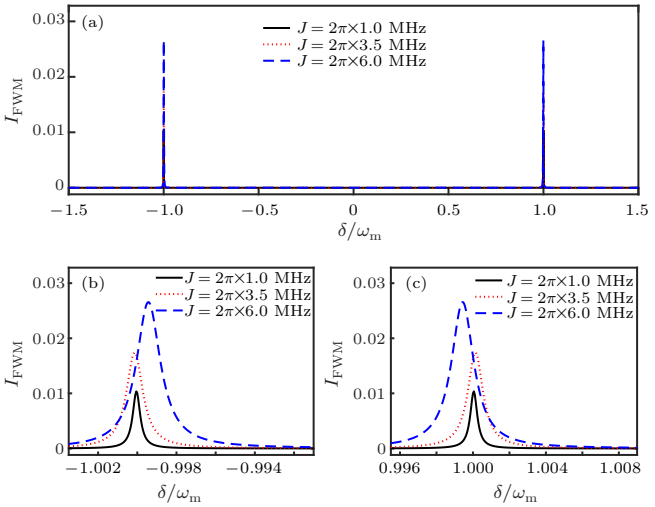


Fig. 3. (a) The FWM intensity $I_{\rm FWM}$ as a function of the probe-pump detuning $\delta/\omega_{\rm m}$ for the case that $P_{\rm p1}=10$ mW and $P_{\rm p2}=0$ with different cavity coupling strength $J=2\pi\times1.0$, $2\pi\times3.5$, and $2\pi\times6.0$ MHz. (b) and (c) are, respectively, the enlarged images of the left and right peaks in (a). Other parameters used are the same as in Fig. 2.

In the following discussions, we mainly consider the case that only the left pump laser is opened. Figures 3 and 4, respectively, present the dependence of the FWM signal on the cavity–cavity coupling strength J and on the atom–cavity coupling strength G for this pump scheme. In Fig. 3(a), the FWM intensity $I_{\rm FWM}$ is plotted as a function of the probe-pump detuning $\delta/\omega_{\rm m}$ for different coupling strength J. Figures 3(b)

and 3(c), respectively, show the enlarged images of the left FWM peak and the right one in Fig. 3(a). It is obvious that with the increase of the coupling strength J both the left and the right peak in the FWM spectrum rise sharply, i.e., the FMW signal is significantly enhanced, and at the same time both peaks suffer a small shift. This phenomenon can be explained as follows. With the increase of the coupling strength between cavity A and B, it will be more and more easy for the pump photons to enter into cavity B, and thus the number of pump photons entering cavity B per second will increase, which will promote the process of FWM generated in cavity B as a result. Moreover, it is well known that increasing the photon number in the cavity can effectively shift the mechanical frequency, so as result the FWM peaks are shifted as well.

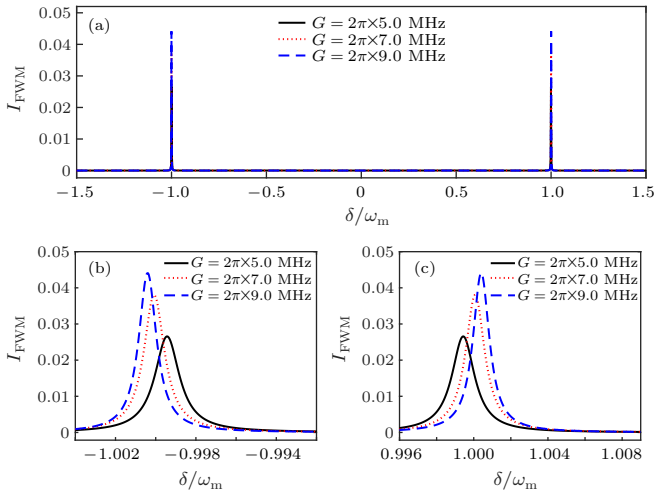


Fig. 4. (a) The FWM intensity $I_{\rm FWM}$ as a function of the frequency detuning $\delta/\omega_{\rm m}$ for different atom-cavity coupling strength $G = 2\pi \times 5.0$, $2\pi \times 7.0$, and $2\pi \times 9.0$ MHz. (b) and (c) are, respectively, the enlarged images of the left and right peaks in (a). Here, $J = 2\pi \times 6.0$ MHz, $P_{\rm p1} = 10$ mW, $P_{\rm p2} = 0$, and other parameters used are the same as in Fig. 2.

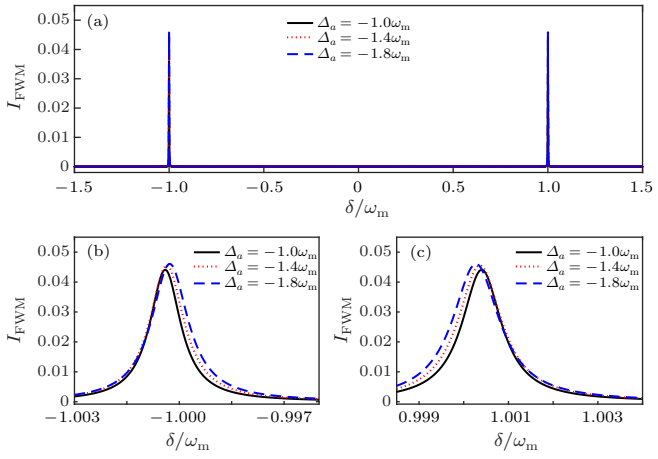


Fig. 5. The FWM intensity $I_{\rm FWM}$ as a function of the frequency detuning $\delta/\omega_{\rm m}$ for atom-pump detuning $\Delta_a < 0$. (b) and (c) are, respectively, the enlarged images of the left and right peaks in (a). Here $J = 2\pi \times 6.0$ MHz, $G = 2\pi \times 9.0$ MHz, $P_{\rm p1} = 10$ mW, $P_{\rm p2} = 0$, and other parameters used are the same as in Fig. 2.

Figure 4 depicts the FWM intensity $I_{\rm FWM}$ as a function of the probe-pump detuning $\delta/\omega_{\rm m}$ for different atom–cavity coupling strength G. This figure clearly shows that the FWM signal generated in cavity B can be significantly strengthened via increasing the atom–cavity coupling strength G in cavity A. In addition, it is obvious that the FWM peaks also have some shift. The phenomena can be attributed to the indirect modulation of cavity A to cavity B. As the atoms interact with the cavity, the distribution of the field intensity in cavity A will be adjusted by the atom–cavity coupling strength. Indirectly, the field intensity of cavity B can also be affected, and as a result the FWM signal generated in cavity B is modulated effectively by the atom–cavity coupling strength.

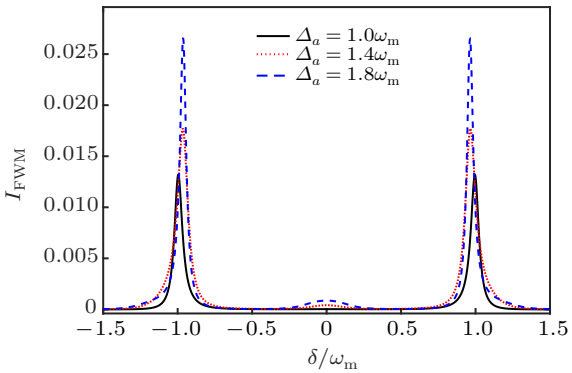


Fig. 6. The FWM intensity $I_{\rm FWM}$ as a function of the frequency detuning $\delta/\omega_{\rm m}$ for atom-pump detuning $\Delta_a > 0$. Other parameters used are the same as in Fig. 5.

Figures 5 and 6 illustrate the FWM intensity $I_{\rm FWM}$ as a function of the probe-pump detuning $\delta/\omega_{\rm m}$ for two opposite detuning case, i.e., $\Delta_a < 0$ and $\Delta_a > 0$. Figure 5 shows that the FWM signal is not sensitive to the atom-pump detuning Δ_a for the blue detuning case, i.e., $\Delta_a < 0$. However, in the opposite case, it is a completely different situation. As shown in Fig. 6, for the red detuning case, i.e., $\Delta_a > 0$, the FWM intensity is enhanced significantly with the increase of the atom-pump detuning Δ_a. Most interestingly, at the resonant region, i.e., $\delta \sim 0$, a prominent peak appears in the FWM spectrum. These phenomena can be easily understood as follows. When the beat frequency δ between the probe and the pump light is approximately equal to the frequency of the mechanical resonator, i.e., $\delta \sim \pm\omega_{\rm m}$, the mechanical mode starts to oscillate coherently, which will induce the generation of FWM.[21] As a result, two strong FWM peaks appear at $\delta \sim \omega_{\rm m}$ and $-\omega_{\rm m}$, respectively, as shown in Figs. 5 and 6. However, at $\delta \sim 0$, it is the resonance between the pump light and the probe light that induces the generation of the FWM. In addition, strong pump light is also needed. It is well known that for $\Delta_a < 0$, the pump light is strongly absorbed by the atoms,[55] so the photon numbers in cavity B is not enough to induce the FWM generation. For $\Delta_a > 0$, the absorption of the atoms is reduced,[55] so more pump photons can enter into cavity B, and as a result the FWM process at $\delta \sim 0$ is opened for this case as shown in Fig. 6.

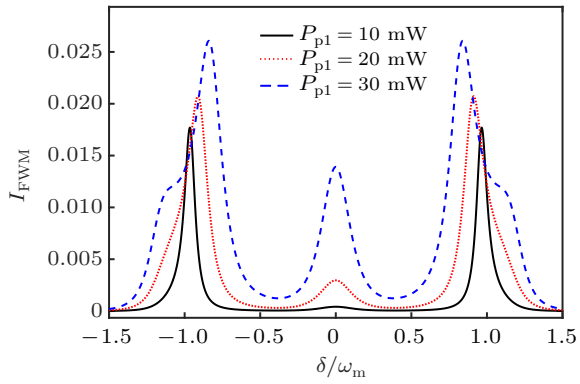


Fig. 7. The FWM intensity I_{FWM} as a function of the frequency detuning δ/ω_m for different pump power $P_{p1} = 10$, 20, and 30 mW. Here, $\Delta_a = 1.4\omega_m$, $J = 2\pi \times 6.0$ MHz, $G = 2\pi \times 9.0$ MHz, $P_{p2} = 0$, and other parameters used are the same as in Fig. 2.

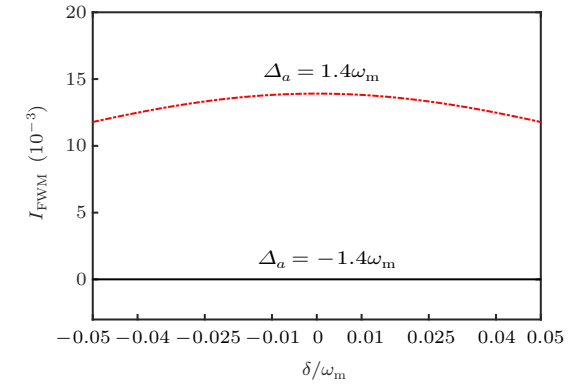


Fig. 8. The FWM intensity I_{FWM} versus the frequency detuning δ/ω_m for different atom-pump detuning Δ_a. Here, $P_{p1} = 30$ mW, $P_{p2} = 0$, $J = 2\pi \times 6.0$ MHz, $G = 2\pi \times 9.0$ MHz, and other parameters used are the same as in Fig. 2.

In Fig. 7, the influence of the pump power on the FWM intensity I_{FWM} for the red detuning case is considered, and the FWM intensity I_{FWM} is plotted as a function of the frequency detuning δ/ω_m for different pump power with $\Delta_a = 1.4\omega_m$. From this figure, it can be clearly observed that as the pump power rises the FWM intensity is largely increased. Importantly, it is obvious that the resonant peak of the FWM intensity at $\delta \sim 0$ is highly sensitive to the pump power, so it is largely improved by the increasing pump power.

The results of Figs. 5–7 show us that this hybrid two-cavity optomechanical system can serve as an all-optical switch.[53,54] To illustrate this idea clearly, Fig. 8 is plotted, which presents the FWM intensity I_{FWM} versus the frequency detuning δ/ω_m for two different atom-pump detunings. When $\Delta_a = -1.4\omega_m$, as is shown in Fig. 8, there is no FWM signal generated in this hybrid system at the resonant region (i.e., $\delta \sim 0$). However, when the atom-pump detuning Δ_a is tuned to $1.4\omega_m$, a prominent FWM signal appears at $\delta \sim 0$. Therefore, this system can act as an all optical switch, and the FWM signal at the resonant region can be easily opened or closed by tuning the atom-pump detuning to be positive or negative.

4. Conclusion

In conclusion, we have theoretically analyzed the FWM effect in a dual-cavity hybrid optomechanical system. First, we propose a mass sensor plan based on this hybrid system for its narrow FWM spectrum, and the numerical results show that the sensitivity and accuracy of the sensor can be improved by adjusting the cavity–cavity or atom–cavity coupling strength. Secondly, we find that the FWM effect at the resonant region can be modulated by controlling the atom-pump detuning to be positive or negative. For this reason, we put forward that the hybrid dual-cavity optomechanical system can be used as an all-optical switch. Finally, we hope that the proposed scheme can be proved experimentally in the near future.

References

[1] Seok H, Buchmann L F, Singh S and Meystre P 2012 *Phys. Rev. A* **86** 063829
[2] Poot M and Zant H S J V D 2012 *Phys. Rep.* **511** 273
[3] Aspelmeyer M, Meystre P and Schwab K 2012 *Phys. Today* **65** 29
[4] Favero I and Karrai K 2009 *Nat. Photon.* **3** 201
[5] Meystre P 2013 *Ann. Phys.* **525** 215
[6] Aspelmeyer M, Kippenberg T J and Marquardt F 2013 *Rev. Mod. Phys.* **86** 1391
[7] Marquardt F and Girvin S M 2009 *Physics* **2** 40
[8] Metzger C H and Karrai K 2004 *Nature* **432** 1002
[9] Kippenberg T J and Vahala K J 2008 *Science* **321** 1172
[10] Aldana S, Bruder C and Nunnenkamp A 2014 *Phys. Rev. A* **90** 063810
[11] Sete E A and Eleuch H 2012 *Phys. Rev. A* **85** 043824
[12] Wang L D, Yan J K, Zhu X F and Chen B 2017 *Phys. E* **89** 134
[13] Chen B, Wang X F, Yan J K and Zhu X F 2018 *Superlattice. Microst.* **113** 301
[14] Bariani F, Seok H, Singh S, Vengalattore M and Meystre P 2015 *Phys. Rev. A* **92** 043817
[15] Chen B, Wang L D, Zhang J and Xue H B 2016 *Phys. Lett. A* **380** 798
[16] Asghari Nejad A, Askari H R and Baghshahi H R 2017 *Chin. Phys. lett.* **34** 084205
[17] Yong H 2016 *Phys. Rev. A* **94** 063804
[18] Mu Q X, Lang C and Zhang W Z 2019 *Chin. Phys. B* **28** 114206
[19] Yong H 2015 *Phys. Rev. A* **91** 013827
[20] Agarwal G S and Huang S 2010 *Phys. Rev. A* **81** 041803
[21] Weis S, Riviere R, Deleglise S, Gavartin E, Arcizet O, Schliesser A and Kippenberg T J 2010 *Science* **330** 1520
[22] Safavi-Naeini A H, Mayer Alegre T P, Chan J, Eichenfield M, Lin Q, Hill J T, Chang D E and Painter 2011 *Nature* **472** 69
[23] Harris S E, Field J E and Imamoglu A 1990 *Phys. Rev. Lett.* **64** 1107
[24] Karuza M, Biancofiore C, Bawaj M, Molinelli C, Galassi M, Natali R, Tombesi P, Giuseppe G D and Vitali D 2013 *Phys. Rev. A* **88** 013804
[25] Yan D, Wang Z H, Ren C N, Gao H, Li Y and Wu J H 2015 *Phys. Rev. A* **91** 023813
[26] Wei W Y, Yu Y F and Zhang Z M 2018 *Chin. Phys. B* **27** 034204
[27] Yan J K, Zhu X F and Chen B 2018 *Chin. Phys. B* **27** 074214
[28] Asghari N A, Askari H R and Baghshahi H R 2017 *Appl. Opt.* **56** 2816
[29] Zhu X F, Wang L D, Yan J K and Chen B 2018 *Optik* **154** 139
[30] Thevenaz L 2008 *Nat. Photon.* **2** 474
[31] Asghari N A, Askari H R and Baghshahi H R 2017 *Chin. Phys. Lett.* **34** 084205
[32] Chang D E, Safavi-Naeini A H, Hafezi M and Painter 2011 *New J. Phys.* **13** 023003
[33] Qiu W, Liu J J, Wang Y D, Yang Y J, Gao Y 2018 *Opt. Commun.* **413** 207
[34] Bigelow M S, Lepeshkin N N and Boyd R W 2003 *Science* **301** 5630
[35] Bigelow M S, Lepeshkin N N and Boyd R W 2003 *Phys. Rev. Lett.* **90** 113903
[36] Wang Y P, Zhang Z C, Yu Y F and Zhang Z M 2019 *Chin. Phys. B* **28** 014202
[37] Jiang C, Cui Y S and Liu H X 2013 *Europhys. Lett.* **104** 34004

[38] Jiang L, Yuan X R, Cui Y S, Chen G B, Zuo F and Jiang C 2017 *Phys. Lett. A* **381** 3289
[39] Wang X F and Chen B 2019 *J. Opt. Soc. Am. B* **36** 162
[40] Chen H J, Wu H W, Yang J Y, Li X C, Sun Y J and Peng Y 2019 *Nanoscale Res. Lett.* **14** 73
[41] Li Z Y, You X, Li Y M, Liu Y C and Peng K C 2018 *Phys. Rev. A* **97** 033806
[42] Li Y Q and Xiao M 1996 *Opt. Lett.* **21** 1064
[43] Deng L, Kozuma M, Hagley E W and Payne M G 2004 *Phys. Rev. Lett.* **88** 143902
[44] Wu Y, Saldana J and Zhu Y 2005 *Phys. Rev. A* **67** 013811
[45] Sun H, Fan S, Zhang H, Zhang H J and Gong S Q 2013 *Phys. Rev. B* **87** 235310
[46] Nielsen M P, Shi X Y, Dichtl P, Maier S A and Oulton R F 2017 *Science* **358** 1179
[47] Li Z P, Wang X L and Li C Y 2016 *Laser Phys. Lett.* **13** 025402
[48] Zhou H, Gu T and Mcmillan J F, Petrone N, Zanda A V D, Hone J C and Yu M B 2014 *Appl. Phys. Lett.* **105** 091111
[49] Ullah K 2019 *Chin. Phys. B* **28** 114209
[50] Huang S and Agarwal G S 2010 *Phys. Rev. A* **81** 033830
[51] Kippenberg T J and Vahala K J 2008 *Science* **321** 1172
[52] Li J J and Zhu K D 2011 *Phys. Rev. B* **83** 245421
[53] Li J J and Zhu K D 2011 *Nanotechnology* **22** 055202
[54] Li J J and Zhu K D 2011 *J. Appl. phys.* **110** 114308
[55] Agarwal G S and Puri R R 1986 *Phys. Rev. A* **33** 1757